Chapter 8
Non-Linear or Quasi-Linear Viscoelastic Property of Blood for Hemodynamic Simulations

Ernesto Romano, Luísa C. Sousa, Carlos C. António, Catarina F. Castro, and Sónia Isabel Silva Pinto

Abstract Hemodynamic simulations with the complex rheology of blood is still a challenge. They can be used to obtain an auxiliary clinical tool, as close as possible to reality, with great potential for the development of preventive measures, diagnosis and treatment of cardiovascular diseases. A wide range of models defining the rheological behavior of blood, ranging from the Newtonian to the purely shear-thinning non-Newtonian models have been used by many authors. However, in vessels, such as carotid or coronary arteries, the validity of such simplified models for blood is not completely clear, mainly in stenotic or aneurysm cases - regions of high velocity gradients. It is well-known, from literature, that blood has complex rheology, behaving as a viscoelastic non-Newtonian fluid due to the storage and release of elastic energy from red blood cells aggregates. Therefore, authors of the present work implemented the viscoelastic property of blood, in UDFs of Ansys® software, in order to simulate the most accurate hemodynamics. Afterwards, the velocity contours, in the middle plane of a 3D idealized coronary artery, were obtained considering the purely shear-thinning model, Carreau model, and two viscoelastic non-Newtonian models. Using the Generalized Oldroyd-B, a quasi-linear model, the viscoelastic effects are not highlighted. Comparing results taking into account the multi-mode Giesekus, a non-linear model, and Carreau model, differences are significant and equal to 0.20 m/s under a maximum velocity of 1.40 m/s (14.3%). Using the multi-mode Giesekus model, the viscoelastic effects are pronounced in addition to the shear-thinning, mainly in regions with high velocity gradients as the stenotic region.

E. Romano, L. C. Sousa, C. C. António, C. F. Castro, S. I. S. Pinto
Engineering Faculty, University of Porto, Porto, Portugal
Institute of Science and Innovation in Mechanical and Industrial Engineering (LAETA-INEGI), Porto, Portugal
e-mail: up201404532@fe.up.pt, lcsousa@fe.up.pt, cantonio@fe.up.pt, ccastro@fe.up.pt, spinto@fe.up.pt

B. E. Abali and I. Giorgio (eds.), *Developments and Novel Approaches in Biomechanics and Metamaterials*, Advanced Structured Materials 132,
https://doi.org/10.1007/978-3-030-50464-9_8

Keywords: Viscoelasticity · Non-linear models · Quasi-linear models · Blood rheology · Hemodynamics

8.1 Introduction

Hemodynamic simulations have proven to be an auxiliary clinical tool with great potential for the development of preventive measures, diagnosis and treatment of cardiovascular diseases. However, the numerical tool should mimic physiological conditions and blood properties as close as possible to reality. There are several models in the literature that can simulate the behavior of blood. Auffray et al (2015) formulated a description for second gradient continua in order to mimic capillary fluids, i.e, fluids for which the deformation energy depends on the second gradient of placement. A Lagrangian action was introduced in both the material and spatial descriptions. The corresponding Euler-Lagrange equations and boundary conditions were found. These conditions were formulated in terms of an objective deformation energy. Eremeyev and Altenbach (2014) have discussed the equilibrium equations and natural boundary conditions also for a second-gradient fluid interacting with a nonlinear elastic solid under finite deformations. They have also taken into account the surface stresses acting at the surface of the solid according to the model. They applied the variational approach based on the energy functional. Rickert et al (2019) have described the flow of fluids with internal rotational degrees of freedom, for example a blood plasma carrying red blood cells (RBC). This blood behavior can be described by the theory of Eringen. Eringen's approach, also known as the micropolar theory of fluids, relies on a consistent use of the complete spin balance and the concept of the conservation of microinertia. They studied such fluids not only from the mechanical point of view, i.e., determining the linear and angular velocities, but also from a thermodynamic one, such as studying the generation of a temperature field during the flow due to internal dissipation. Thus, this requires the balance of momentum, spin and internal energy in combination.

Many authors specialized, concretely, in cardiovascular engineering field have used a wide range of models defining the rheological behavior of blood, ranging from the Newtonian to the purely shear-thinning non-Newtonian models. The particles are oriented randomly in the minimum energy states and the RBC in plasma undergo reversible aggregation, the rouleaux (Thanapong Chaichana, Zhonghua Sun, 2012; De Santis et al, 2013; Lee et al, 2008; Morbiducci et al, 2011; Van Canneyt et al, 2013). However, in vessels, such as carotid or coronary arteries, the validity of the Newtonian and the purely shear-thinning non-Newtonian hypotheses is not completely clear, mainly in stenotic or aneurysm cases – regions of high velocity gradients. It is well-known from literature that blood has a viscoelastic non-Newtonian behavior (Baskurt and Meiselman, 2003; Bodnár et al, 2011; Campo-Deaño et al, 2013, 2015) due to the storage and release of elastic energy from RBC aggregates.

Baskurt and Meiselman (2003) have described the way in which blood viscosity is affected by hematocrit, shear rate and red blood cells aggregation. They also emphasize the importance of red blood cell deformability and list factors which affect the cellular mechanical property. Campo-Deaño et al (2013) achieved, experimentally, several parameters, namely the mobility factor and the extensibility coefficient, for viscoelastic non-Newtonian models of blood at 37°C –the multi-mode Giesekus and simplified Phan-Thien-Tanner (sPTT) models. Later, Campo-Deaño et al (2015) presented a state-of-the-art review of the different models used in the hemodynamics, focusing on modeling blood as a viscoelastic non-Newtonian fluid, in order to understand the role of the complex rheology of blood upon the dynamics in aneurysms.

Nevertheless, few authors have considered the viscoelastic property of blood in numerical simulations. Bodnár et al (2011) demonstrated and quantified the most relevant non-Newtonian characteristics of blood flow in vessels, namely its shear-thinning and viscoelastic behavior. Numerical simulations, through a finite-volume method, were performed in a 3D idealized stenosed vessel, with nominal vessel diameter equal to 6.2 mm. Four models for blood were taken into account: the Newtonian (NS) and the Generalized Newtonian (GNS) models; and the Oldroyd-B (OB) and the Generalized Oldroyd-B (GOB) models. The NS model assumes constant viscosity of blood at infinite shear rate, the GNS considers fluid with variable shear-thinning viscosity, OB takes into account the elastic property of blood and constant viscosity at infinite shear rate and GOB assumes the elastic property of blood with variable shear-thinning viscosity. At constant flow rate, the impact of non-Newtonian effects was observed and viscoelasticity of blood was highlighted. Therefore, simulations considering the complex rheology of blood, viscoelasticity, are of great interest since the most accurate hemodynamic is essential for clinical practice. There is a need for the use of models depicting this behavior.

Thus, authors of the present paper want to take a step forward in the numerical hemodynamic simulations through the implementation and validation of a more accurate rheological model for blood in *User-Defined Functions* (UDF) associated to the *Ansys*® software package. *Ansys*® software was chosen since it is a user-friendly software, widely used by other authors. So that, the UDFs implemented by authors of the present paper can be, in the future, easily used by other authors.

In the present work, a 3D idealized geometry of a stenosed bifurcation, mimicking a right coronary artery (RCA) bifurcation, was chosen to show the accuracy of using the implemented viscoelastic models. Two different viscoelastic non-Newtonian models also able to predict shear-thinning behavior - a Generalized Oldroyd-B model, a quasi-linear model (Bird et al, 1987), and a multi-mode Giesekus model, a non-linear model (Larson, 1988) - were compared with a simpler Generalized Newtonian model – Carreau Model. For all models, time-dependent velocity and pressure profiles of pulsatile flow and pressure waveforms, characteristics of a right coronary artery, were imposed as boundary conditions for numerical simulations.

8.2 Materials and Methods

8.2.1 Mathematical Models for Blood Rheology

The governing equations, taking into account the principles of mass conservation and linear momentum conservation for an incompressible fluid, used in blood flow dynamics, can be defined by:

$$\begin{gathered} \nabla \cdot \mathbf{u} = 0 \\ \rho \left(\frac{\partial \mathbf{u}}{\partial t} + \mathbf{u} \cdot \nabla \mathbf{u} \right) = -\nabla p + \nabla \cdot \boldsymbol{\tau} \end{gathered} \tag{8.1}$$

where $\mathbf{u}$ is the velocity vector, ρ the blood density, p the pressure, t the instant time and $\boldsymbol{\tau}$ the extra stress tensor. These governing equations can also describe fluids with viscoelastic non-Newtonian behavior using a constitutive equation defining $\boldsymbol{\tau}$.

Generally, the total stress $\boldsymbol{\tau}$ is expressed by the sum of the solvent part $\boldsymbol{\tau}_s$ and the elastic part $\boldsymbol{\tau}_e$:

$$\boldsymbol{\tau} = \boldsymbol{\tau}_s + \boldsymbol{\tau}_e \tag{8.2}$$

where $\boldsymbol{\tau}_s$ is equal to:

$$\boldsymbol{\tau}_s = 2\mu_s \mathbf{D} \tag{8.3}$$

depending on the viscosity of the solvent part (μ_s) and the strain rate tensor ($\mathbf{D}$).

The elastic stress, $\boldsymbol{\tau}_e$, satisfies the following equations:

$$\begin{gathered} f(\boldsymbol{\tau}_e)\boldsymbol{\tau}_e + \lambda \overset{\triangledown}{\boldsymbol{\tau}}_e + \alpha \frac{\lambda}{\mu_e}(\boldsymbol{\tau}_e \cdot \boldsymbol{\tau}_e) = 2\mu_e \mathbf{D} \\ f(\boldsymbol{\tau}_e) = 1 + \frac{\lambda \varepsilon}{\mu_e} tr(\boldsymbol{\tau}_e) \end{gathered} \tag{8.4}$$

where μ_e is the viscosity related to the elastic part of the fluid, α is the mobility factor, ε the extensibility coefficient and $\overset{\triangledown}{\boldsymbol{\tau}}_e$ is the upper-convected derivative in the elastic contribution of the extra stress tensor.

Since blood has complex rheology, three models were considered in order to observe the importance of considering the viscoelasticity of blood in the hemodynamics. The simplest model chosen is a Generalized Newtonian Model, purely shear-thinning model (without viscoelasticity), through Carreau Model:

$$\mu_s(\dot{\gamma}) = \mu_\infty + (\mu_0 - \mu_\infty) \times [1 + (\lambda \dot{\gamma})^2]^{\frac{n-1}{2}} \tag{8.5}$$

In this model, $\boldsymbol{\tau}$ is equal to $\boldsymbol{\tau}_s$ and $\boldsymbol{\tau}_e$ is equal to 0. μ_s is the viscosity of the solvent part and $\dot{\gamma}$ the shear rate. For blood at 37°C, the viscosity at infinite shear rate (μ_∞) is equal to 0.00345 Pa s, the viscosity at zero shear rate (μ_0) equal to 0.056 Pa s, the relaxation time (λ) is 3.313 s and the power index (n) equal to 0.3568 (Johnston et al, 2004).

Two different viscoelastic non-Newtonian models were used to also predict the shear-thinning behavior of blood: the Generalized Oldroyd-B model and the multi-mode Giesekus model.

The Generalized Oldroyd-B considers both the mobility factor (α) and the extensibility coefficient (ε) of Equation (8.4) equal to 0 – a quasi-linear model (Bird et al, 1987). Thus, the constitutive equation becomes:

$$\boldsymbol{\tau}_e + \lambda \overset{\triangledown}{\boldsymbol{\tau}}_e = 2\mu_e \mathbf{D} \tag{8.6}$$

The viscosity related to the elastic part (μ_e) is equal to 4.0×10^{-6} Pa s and the relaxation time (λ) is 0.06 s, for blood (Bodnár et al, 2011). The shear-thinning viscosity (μ_s) was defined through Carreau Model represented by Equation (9.8) and parameters for blood are the same as defined previously (Johnston et al, 2004).

The Giesekus model, defining viscoelasticity and shear-thinning, was used in multi-mode form. Each mode number is defined by k. The viscoelastic multi-mode Giesekus model does not take into account the extensibility coefficient (ε) of Equation (8.4) ($\varepsilon = 0$). However, the model considers the mobility factor (α). Therefore, the viscoelastic multi-mode Giesekus model is a non-linear model (Larson, 1988) represented by:

$$\boldsymbol{\tau}_{e_k} + \lambda_k \overset{\triangledown}{\boldsymbol{\tau}}_{e_k} + \frac{\alpha_k \lambda_k}{\mu_{e_k}} (\boldsymbol{\tau}_{e_k} \cdot \boldsymbol{\tau}_{e_k}) = 2\mu_{e_k} \mathbf{D} \tag{8.7}$$

The total elastic stress ($\boldsymbol{\tau}_e$) is the sum of the elastic stress of each k mode ($\boldsymbol{\tau}_{e_k}$) in the total of m modes.

$$\boldsymbol{\tau}_e = \sum_{k=1}^{m} \boldsymbol{\tau}_{e_k} \tag{8.8}$$

Parameters of the multi-mode Giesekus for whole human blood were obtained experimentally by Campo-Deaño et al (2013) and can be shown in Table 9.1.

In addition to the shear-thinning and viscoelastic property of blood, blood was also considered as isotropic, incompressible and homogeneous fluid with constant density (ρ = 1060 kg/m^3).

Table 8.1 Parameters of the multi-mode Giesekus model for human blood (Campo-Deaño et al, 2013)

Mode	μ_{e_k} $[Pa \cdot s]$	λ_k $[s]$	α_k
1	0.05	7	0.06
2	0.001	0.4	0.001
3	0.001	0.04	0.001
4	0.0016	0.006	0.001
Solvent	$\mu_s = 0.0012\,\mathrm{Pa\,s}$		

8.2.2 Implementation of the Viscoelastic Models

The previous viscoelastic models are not included in *Ansys® Fluent* package. However, they can be implemented through *user-defined-functions* (UDFs). UDFs are functions or subroutines programmed in a modified C language which are loaded in *Ansys® Fluent*. This software was used in the present work, to implement the viscoelastic models for blood and further hemodynamic simulations, since it is a user-friendly software widely used by other authors. Therefore, the UDFs implemented by authors of the present paper can be, in the future, easily manipulated by other authors.

The Einstein notation was used in order to compact extensive equations. Einstein notation implies the sum of a set of indexed terms in a formula. In the current case, the subscript *n* must be replaced for a sum of the different Cartesian components, i.e, *x, y* and *z*. Thus, the upper-convected derivative equation becomes:

$$\overset{\triangledown}{\tau}_{ij_k} = \frac{\partial \tau_{ij_k}}{\partial t} + u_n \frac{\partial \tau_{ij_k}}{\partial x_n} - \tau_{nj_k} \frac{\partial u_i}{\partial x_n} - \tau_{in_k} \frac{\partial u_j}{\partial x_n} \tag{8.9}$$

Adding Eq. (8.9) to Eq. (9.6), the equation with the upper convected derivative terms on the left side was obtained:

$$\begin{aligned} \frac{\partial \tau_{ij_k}}{\partial t} + u_n \frac{\partial \tau_{ij_k}}{\partial x_n} - \tau_{nj_k} \frac{\partial u_i}{\partial x_n} - \tau_{in_k} \frac{\partial u_j}{\partial x_n} = \frac{2\mu_{e_k} D_{ij}}{\lambda_k} - \\ \frac{1}{\lambda_k} f(\tau_{ij_k}) \tau_{ij_k} - \frac{\alpha_k}{\mu_{e_k}} (\tau_{in_k} \cdot \tau_{nj_k}) \end{aligned} \tag{8.10}$$

Eq. (8.10) can be simplified as:

$$\frac{\partial \tau_{ij_k}}{\partial t} + u_n \frac{\partial \tau_{ij_k}}{\partial x_n} = S_{\tau_{ij_k}} \tag{8.11}$$

where $S_{\tau_{ij_k}}$ are the source terms for each stress component, and for each mode, defined as:

$$S_{\tau_{ij_k}} = \frac{2\mu_{e_k} D_{ij}}{\lambda_k} - \frac{1}{\lambda_k} f(\tau_{ij_k})\tau_{ij_k} - \frac{\alpha_k}{\mu_{e_k}}(\tau_{in_k} \cdot \tau_{nj_k}) + \tau_{nj_k}\frac{\partial u_i}{\partial x_n} + \tau_{in_k}\frac{\partial u_j}{\partial x_n} \tag{8.12}$$

The last step of the implementation was the analysis of the Navier–Stokes equations. The basic conversion of the moment equation must be modified in order to include the decomposition of the stress tensor (Eq. (8.10)). As such, there is a need to take into account the elastic parts of the stress, which are calculated as scalars. This was achieved through the addition of the divergence of the extra stress tensor, $\boldsymbol{\tau}_e$, as sources to the momentum equations, known in *Ansys® Fluent* as momentum sources.

$$\begin{aligned} S_{M_x} &= \sum_{k=1}^{m} \frac{\partial \tau_{xn_k}}{\partial x_n} \\ S_{M_y} &= \sum_{k=1}^{m} \frac{\partial \tau_{yn_k}}{\partial x_n} \\ S_{M_z} &= \sum_{k=1}^{m} \frac{\partial \tau_{zn_k}}{\partial x_n} \end{aligned} \tag{8.13}$$

8.2.3 3D Geometry and Computational Mesh

A 3D idealized geometry representing a bifurcation of a RCA was constructed in *Solidworks®* (Fig. 9.1a). The main branch representing a RCA starts with 3 mm diameter and after bifurcation decreases to 2.5 mm. The side-branch, with much lower diameter than the main branch, was considered to have a 1.5 mm diameter. A 40% lumen stenosis in the main branch just after the bifurcation was also designed in order to observe the viscoelastic effects in these regions of flow acceleration and recirculation.

The 3D idealized geometry with the inlet and outlet boundaries perpendicular to the blood flow, and the axis defined at the inlet, was imported to *Meshing Ansys®* to construct the computational mesh.

A tetrahedral mesh was defined in all the domain of the artery (Fig. 9.1b). The *Path Independent Method of Meshing Ansys®* was selected in order to uniform the elements and to obtain an accurate mesh (Ansys, 2013). So, the statistical parameter *Skewness* was used to verify the precision of the mesh. A *Maximum Skewness* of 0 indicates the best case scenario, equilateral cells, while a *Maximum Skewness* equal of 1 indicates the worst case scenario, completely degenerated cells. Following the tutorial guide of *Ansys®*, the mesh is accurate when the *Maximum Skewness* is lower than 0.95 (Ansys, 2013). The computational mesh of this work has a *Maximum*

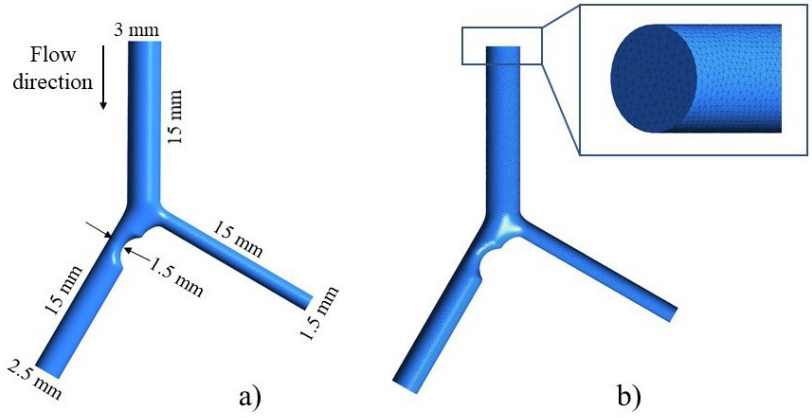

Fig. 8.1 (a) 3D geometry of the idealized RCA constructed in *SolidWorks*®; (b) 3D computational mesh obtained through *Meshing Ansys*® software.

Skewness equal to 0.58 with 182909 elements, which is considered accurate for numerical simulations.

8.2.4 Boundary Conditions

Boundary conditions must be imposed. At the inlet of the idealized geometry, a Womersley velocity profile was taken into account. This profile depends on the instant time of the cardiac cycle, the radial position at the inlet and the Womersley number:

$$W_o = R\sqrt{\frac{\rho\omega}{\mu}} \tag{8.14}$$

The Womersley number (W_o) is defined by the radius of the artery (R), the blood density (ρ), the viscosity of blood (μ) at infinite shear rate and the cardiac frequency (ω). For the present geometry, W_o is equal to 2.40 corresponding to an inlet diameter of the artery equal to 3 mm. At the outlet branches, pressure profiles were imposed. These profiles are dependent on the instant time of the cardiac cycle but radius-independent.

The boundary conditions, defined previously, for RCAs, were also implemented in UDFs in *Ansys*® software by some authors of the present paper (Pinho et al, 2019a,b). Fig. 9.2 shows the mean velocity profile imposed at the inlet of the idealized artery and the pressure profile at the outlet branches.

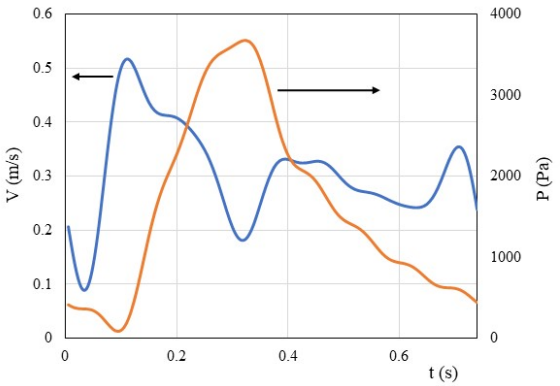

Fig. 8.2 Mean velocity profile imposed at the inlet of the idealized RCA (blue line) and pressure profile imposed at the outlet branches (orange line).

8.2.5 Numerical Method

Ansys® *Fluent* software was used to perform computational fluid dynamic (CFD) simulations of unsteady blood flow. Navier–Stokes equations were solved in a laminar regime, since Reynolds number in the systolic peak does not exceed the value of 1000. The velocity-pressure coupled equations were solved by the SIMPLE algorithm. The momentum equations with the implemented source terms were discretized by the second-order upwind scheme. The analysis was performed considering a total time of the cardiac cycle equal to 0.74 s, using 148 times steps, each one equal to 0.05 s; the number of iterations for each time step was equal to 20. The simulation process was completed according the convergence criteria of 1×10^{-4}.

8.3 Results and Discussion

Fig. 9.3 represents the velocity contours, in the systolic peak (maximum velocity of the cardiac cycle), along the middle plane of the 3D idealized coronary geometry, for three different rheological models: a Generalized Newtonian model, purely shear-thinning model, through Carreau model; and two viscoelastic non-Newtonian models as the Generalized Oldroyd-B and the multi-mode Giesekus.

For the three cases, there is an acceleration of blood flow in the stenotic region, where the maximum velocity is 1.40 m/s, and there are also recirculation regions just after the stenosis. However, Fig. 9.3 shows that the effect of the viscoelastic components of stress decreases the velocity of blood flow in the stenosis and increases the velocity in the recirculation regions. This effect is highlighted considering the multi-mode Giesekus model.

The Generalized Oldroyd-B model assumes that both mobility factor and extensibility coefficient are equal to 0 and only one mode. It is considered a quasi-linear model (Bird et al, 1987). The multi-mode Giesekus model takes into account four

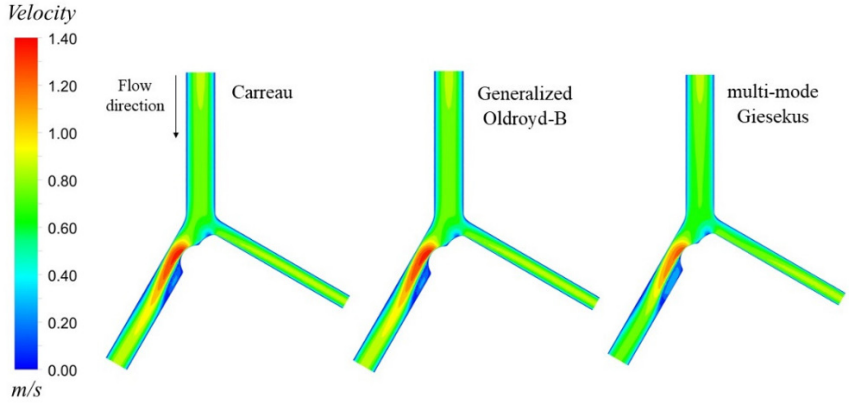

Fig. 8.3 Velocity contours, in the systolic peak, along the middle plane of the 3D idealized coronary geometry for the different rheological models.

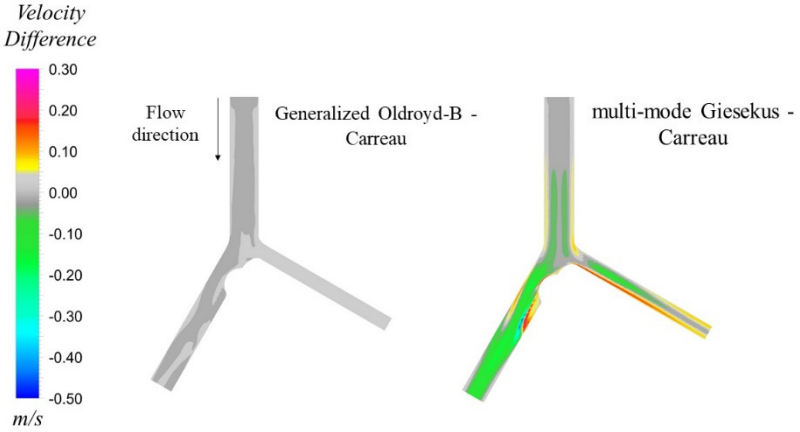

Fig. 8.4 Velocity difference between the Viscoelastic models (Generalized Oldroyd-B and multi-mode Giesekus) and the Generalized Newtonian model (Carreau), in the systolic peak.

modes with four different mobility factors (only the extensibility coefficient equal to 0). This model is a non-linear model (Larson, 1988). Therefore, Fig. 9.4 shows that velocity differences considering the Generalized Oldroyd-B model (quasi-linear viscoelastic model) and Carreau model are almost null (grey region), which means that viscoelastic effects using Generalized Oldroyd-B for blood are not so pronounced. These conclusions are in concordance with those of Bodnár et al (2011). Bodnár et al (2011) consider a different geometry and different boundary conditions (constant flow rate); however, they also concluded that for a higher flow rate, equal to 2 cm^3/s, velocities almost overlap considering these two models. In the present paper, the velocities are also almost coincident for a maximum flow rate, in the systolic peak, equal to 3.9 cm^3/s.

Differences in velocity between using the multi-mode Giesekus and Carreau model are highlighted in Fig.9.4, where the viscoelasticity effects are well evident. The green regions, velocity differences around -0.20 m/s, mean that resulted velocities from simulations taking into account Carreau model are 0.20 m/s higher than using multi-mode Giesekus. In the recirculation regions, the opposite happens. In Fig.9.4, a velocity difference of 0.20 m/s (red regions) can be observed, meaning that velocity field using multi-mode Giesekus is higher than using Carreau model, in the recirculation region. These differences are significant, mainly in regions with high velocity gradients as stenotic regions, in a scale with maximum value of 1.40 m/s. Such results are not surprising since multi-mode Giesekus model is a non-linear model and well-known as one of the best to characterize viscoelastic fluids (Bird et al, 1987).

8.4 Conclusion

The viscoelastic non-Newtonian models, the Generalized Oldroyd-B and multi-mode Giesekus, characterizing the complex rheology of blood for accurate hemodynamic simulations, were implemented in UDFs in *Ansys*® software. The velocity contours, in the middle plane of a 3D idealized right coronary artery, were plotted considering the purely shear-thinning model, Carreau model, and the two viscoelastic non-Newtonian models. Using the Generalized Oldroyd-B and Carreau model, differences are almost null, meaning that the viscoelastic effects in Generalized Oldroyd-B are not pronounced. This model is a quasi-linear model. These results are in concordance with those obtained in literature. Comparing results considering multi-mode Giesekus and Carreau model, differences are significant and equal to 0.20 m/s under a maximum velocity of 1.40 m/s (14.3%). Using the multi-mode Giesekus model, the viscoelastic effects are highlighted in addition to the shear-thinning, mainly in regions with high velocity gradients as the stenotic region. Whether the viscoelastic models are emphasized in idealized geometry bifurcations, where the velocity gradients of flow are high, the same viscoelastic models will certainly be accurate in real models of arteries.

Acknowledgements Authors gratefully acknowledge the funding by *Fundação para a Ciência e Tecnologia* (FCT), Portugal, through the funding of the "Associated Laboratory of Energy, Transports and Aeronautics (LAETA)", UID/EMS/50022/2019, the Institute of Science and Innovation in Mechanical and Industrial Engineering (LAETA-INEGI), the Engineering Faculty of University of Porto (FEUP), the Cardiovascular R&D Unit of the Medicine Faculty of University of Porto (FMUP) and the Cardiology Department of Gaia/Espinho Hospital Centre.

References

Ansys (2013) Ansys Academic 16.0. ANSYS Fluent Tutorial Guide

Auffray N, dell'Isola F, Eremeyev VA, Madeo A, Rosi G (2015) Analytical continuum mechanics à la Hamilton–Piola least action principle for second gradient continua and capillary fluids. Mathematics and Mechanics of Solids 20(4):375–417

Baskurt OK, Meiselman HJ (2003) Blood rheology and hemodynamics. Seminars in thrombosis and hemostasis 29(5):435–450

Bird R, Armstrong R, Hassager O (1987) Dynamics of Polymeric Liquids, Volume 1: Fluid Mechanics, 2nd edn. John Wiley and Sons Inc

Bodnár T, Sequeira A, Prosi M (2011) On the shear-thinning and viscoelastic effects of blood flow under various flow rates. Applied Mathematics and Computation 217(11):5055–5067

Campo-Deaño L, Dullens RPA, Aarts DGAL, Pinho FT, Oliveira MSN (2013) Viscoelasticity of blood and viscoelastic blood analogues for use in polydymethylsiloxane in vitro models of the circulatory system. Biomicrofluidics 7(3):34,102

Campo-Deaño L, Oliveira M, T Pinho F (2015) A Review of Computational Hemodynamics in Middle Cerebral Aneurysms and Rheological Models for Blood Flow. Applied Mechanics Reviews 67(3):30,801

De Santis G, Conti M, Trachet B, De Schryver T, De Beule M, Degroote J, Vierendeels J, Auricchio F, Segers P, Verdonck P, Verhegghe B (2013) Haemodynamic impact of stent-vessel (mal)apposition following carotid artery stenting: mind the gaps! Computer methods in biomechanics and biomedical engineering 16(6):648–659

Eremeyev VA, Altenbach H (2014) Equilibrium of a second-gradient fluid and an elastic solid with surface stresses. Meccanica 49(11):2635–2643

Johnston BM, Johnston PR, Corney S, Kilpatrick D (2004) Non-Newtonian blood flow in human right coronary arteries: steady state simulations. Journal of biomechanics 37(5):709–720

Larson RGBT (1988) Constitutive Equations for Polymer Melts and Solutions. In: Larson RGBT (ed) Butterworths Series in Chemical Engineering, Butterworth-Heinemann

Lee SW, Antiga L, Spence JD, Steinman DA (2008) Geometry of the carotid bifurcation predicts its exposure to disturbed flow. Stroke 39(8):2341–2347

Morbiducci U, Gallo D, Massai D, Ponzini R, Deriu MA, Antiga L, Redaelli A, Montevecchi FM (2011) On the importance of blood rheology for bulk flow in hemodynamic models of the carotid bifurcation. Journal of biomechanics 44(13):2427–2438

Pinho N, Castro CF, António CC, Bettencourt N, Sousa LC, Pinto SIS (2019a) Correlation between geometric parameters of the left coronary artery and hemodynamic descriptors of atherosclerosis: FSI and statistical study. Medical & biological engineering & computing 57(3):715–729

Pinho N, Sousa LC, Castro CF, António CC, Carvalho M, Ferreira W, Ladeiras-Lopes R, Ferreira ND, Braga P, Bettencourt N, Pinto SIS (2019b) The Impact of the Right Coronary Artery Geometric Parameters on Hemodynamic Performance. Cardiovascular engineering and technology 10(2):257–270

Rickert W, Vilchevskaya E, Müller W (2019) A note on Couette flow of micropolar fluids according to Eringen's theory. Mathematics and Mechanics of Complex Systems 7(1):25–50

Thanapong Chaichana, Zhonghua Sun JJ (2012) Computational Fluid Dynamics Analysis of the Effect of Plaques in the Left Coronary Artery. Computational and Mathematical Methods in Medicine 2012:9

Van Canneyt K, Morbiducci U, Eloot S, De Santis G, Segers P, Verdonck P (2013) A computational exploration of helical arterio-venous graft designs. Journal of biomechanics 46(2):345–353